Biomineral-inspired growth of metal-organic frameworks in gelatin hydrogel matrices

ARTICLE *in* JOURNAL OF MATERIALS CHEMISTRY · AUGUST 2013

Impact Factor: 7.44 · DOI: 10.1039/C3TB20814A

4 AUTHORS, INCLUDING:

Ashesh Garai
University of Southampton
20 PUBLICATIONS **535** CITATIONS
SEE PROFILE

Jia Huo
Hunan University
51 PUBLICATIONS **643** CITATIONS
SEE PROFILE

Darren Bradshaw
University of Southampton
58 PUBLICATIONS **4,648** CITATIONS
SEE PROFILE

Journal of Materials Chemistry B

RSC Publishing

PAPER

View Article Online
View Journal

Cite this: DOI: 10.1039/c3tb20814a

Biomineral-inspired growth of metal–organic frameworks in gelatin hydrogel matrices†

Ashesh Garai, William Shepherd, Jia Huo and Darren Bradshaw*

Received 7th June 2013
Accepted 12th June 2013

DOI: 10.1039/c3tb20814a

www.rsc.org/MaterialsB

In this work we employ a biomineral-inspired growth approach to the prototypical metal–organic frameworks (MOFs) ZIF-8 and HKUST-1 using cheap abundant non-toxic gelatin hydrogels as both a matrix and macromolecular additive for crystal growth. Both MOFs are readily prepared within the hydrogel, and while ZIF-8@gelatin composites are readily dispersed in water to form colloidal solutions stable for several months, the matrix has a significantly more pronounced effect on the crystal growth and morphology of HKUST-1 directly mirroring natural matrix-mediated biomineralisation processes. Addition of small amounts of gelatin (<1 wt%) to solvothermal syntheses of the frameworks indicates that the biomacromolecule can influence particle size, and in the case of HKUST-1 leads to mesostructured aggregates of particles that can be tuned across multiple length scales.

Introduction

Biomineralisation is the process by which inorganic minerals are incorporated into biological systems. When mineralisation is under strict biological control this highly regulated process produces composite materials with unprecedented levels of structural complexity and finely tuned mechanical properties for specialist biological functions.[1] The mechanisms that permit such high levels of control typically involve interaction between the mineral phase and a functional organic interface. Matrix-mediated biomineralisation for example exploits pre-formed supramolecular assemblies of proteins, polysaccharides or glycoproteins that compartmentalize mineralisation space within fibrous hydrated networks that act as functional and structural frameworks to direct nucleation and crystal growth/orientation. While this is clearly complex, the growth of crystals in biological and synthetic hydrogels is a versatile platform to model such processes and exert control over crystal size, morphology and polymorph selection of biologically prevalent mineral phases such as calcium carbonate[2] and fluoro-[3] and hydroxyapatite.[4] In this report we extend this bioinspired approach to the preparation of hybrid metal–organic framework (MOFs) crystals in hydrogels.

MOFs are microporous materials formed by the assembly of metal ions or clusters and multitopic organic linkers[5] and are characterised by their tuneable pore sizes and functionality ensuring they have broad application in gas storage, separation, catalysis and drug delivery.[6] There is currently a significant drive to prepare MOFs at the nanoscale and with some degree of shape control[7] to further extend their reach and provide a basis for their incorporation into functional devices. Nanoscale MOFs have been prepared using microemulsions, interfacial synthesis in microfluidic devices, microwave and sonochemical methods and by the delamination of thin films.[7,8] Small molecule coordination modulators are also widely employed as growth inhibitors to limit MOF crystal size,[7,8] and in some cases can lead to anisotropic crystal growth.[9] On the other hand, the use of soluble biologically derived organic macromolecules as scaffolds[10] or additives for MOF growth is largely unexplored, despite the advantages this offers in terms of processability, dispersibility, morphology control and biocompatibility. While a recent patent[11] details the preparation of MOF–biopolymer composites by dispersion of pre-formed MOF particles in polysaccharide solutions, here we demonstrate a true bioinspired growth approach of the prototypical MOFs $Zn(2\text{-MeIm})_2$ ZIF-8[12] and $Cu_3(BTC)_2(H_2O)_3$ HKUST-1[13] (2-MeIm = 2-methylimidazole; BTC = 1,3,5-benzenetricarboxylate) *in situ* within gelatin hydrogel matrices.

Experimental

General

Gelatin (G2500), zinc(II) nitrate hexahydrate (96482), 2-methylimidazole (M50850), copper(II) acetate monohydrate (25038) and trimesic acid (482749) were all purchased from Sigma-Aldrich. All composite hydrogel syntheses were conducted in MilliQ water.

Synthesis

Preparation of 5 wt% gelatin pellets. A 5 wt% gelatin solution was prepared by dissolving 250 mg of gelatin in 5 ml water at 60 °C and holding at this temperature for 2 h. The solution

School of Chemistry, University of Southampton, Highfield, Southampton SO17 1BJ, UK. E-mail: D.Bradshaw@soton.ac.uk; Tel: +44 (0)23 8059 9076

† Electronic supplementary information (ESI) available: Additional characterisation data. See DOI: 10.1039/c3tb20814a

was pipetted into partially sealed drinking straws (dia 4 mm) and cooled in a refrigerator for 2 h to set the gel. The straws were cut into 20 lengths of 1 cm for use.

ZIF-8@gelatin composites. Two procedures were followed as indicated in Scheme 1.

Route (a). 10 pellets of pure gelatin were placed into 10 ml of aqueous $Zn(NO_3)_2 \cdot 6H_2O$ (0.0168 M) and soaked overnight. After washing 3 times with fresh water, the pellets were placed into 10 ml ethanolic solution of 2-methylimidazole (0.672 M). After standing overnight, the resulting ZIF-8@gelatin composite pellets were washed 3 times with ethanol and water respectively and freeze dried for characterisation.

Route (b). Zn(II)@gelatin precursor pellets were prepared by mixing 100 mg (0.336 mmol) $Zn(NO_3)_2 \cdot 6H_2O$ and 250 mg gelatin in 5 ml water at 60 °C. This solution was cast in drinking straws as previously described. 10 pellets of Zn(II)@gelatin were placed into 10 ml ethanolic solution of 2-methylimidazole (0.672 M). After standing overnight, the resulting ZIF-8@gelatin composite pellets were washed and freeze-dried as for route (a). Precursor gels containing 5, 10, 20, 30 and 40 mg of $Zn(NO_3)_2 \cdot 6H_2O$ were also prepared in the same way.

Redispersion of ZIF-8@gelatin. 1–2 slices of ZIF-8@gelatin pellets (prepared by route (b)) were redispersed into 10 ml water and left to stand for two months under ambient conditions to determine their dispersion stability. For DLS measurements, the dispersions were further diluted with water.

HKUST-1@gelatin composites (route (a)). 10 pellets of pure gelatin were soaked overnight in 10 ml of an aqueous solution of $Cu(OAc)_2 \cdot H_2O$ (0.015 M). The Cu(II)@gelatin pellets were washed 3 times with water before further soaking overnight in an aqueous solution of trimesic acid (0.02 M) and 3 equivalents of NaOH. The resulting HKUST-1@gelatin pellets were washed 3 times with ethanol and freeze dried prior to analysis.

Removal of gelatin from ZIF-8@gelatin composites. ZIF-8@gelatin composite pellets were placed into water (20 ml) and heated at 90 °C for an initial period of 24 h. The resulting solid was recovered by centrifugation at 12 500 rpm, re-suspended in water (20 ml) and further heated at 90 °C for 6 h. The solid was recovered as before and this step repeated 4 times. The solid was finally collected, washed with EtOH (5 ml), and dried at RT.

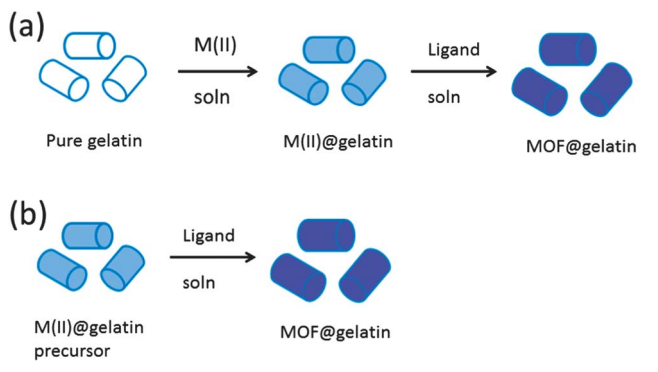

Scheme 1 Illustration of the two routes employed for the growth of metal–organic frameworks within gelatin hydrogels as exemplified for HKUST-1 growth.

Gelatin as a macromolecular additive. ZIF-8 and HKUST-1 were both prepared under solvothermal conditions at 120 °C for 12 h in the presence of small amounts of added gelatin. ZIF-8 was synthesised wholly in aqueous solution with a Zn : 2-MeIm ratio of 1 : 40, and HKUST-1 in a 50 : 50 EtOH–H_2O solvent mixture with a Cu : BTC ratio of 1 : 1 or 3 : 2.

Characterisation methods

The morphology of the freeze dried gels was recorded in a field emission scanning electron microscope (FE-SEM) apparatus (Hitachi S-4800). The samples were gold coated and were observed at a voltage of 5 kV. For TEM, a drop of the dispersed aqueous solution was placed on a carbon-coated Cu grid and observed through a transmission electron microscope (FEI Tecnai G2 Spirit BioTWIN) at an accelerated voltage of 120 kV. The structure of the MOF@gelatin composites was confirmed using a Bruker powder diffractometer in transmission mode with monochromated Cu Kα1 radiation (λ = 0.154 nm) operating at 35 kV and 30 mA. The thermal stability of the samples were measured using a TGA/DTA instrument (model SDT Q600, TA instrument) under a flowing air atmosphere at a heating rate of 10 °C min^{-1} up to 800 °C. Rheological experiments were carried out using a stress-controlled Anton Paar Physica MCR101 rheometer using a parallel plate geometry and solvent trap setup. The plate diameter was 20 mm and the plate gap was 500 μm. The experiments were conducted over the temperature range 15–80 °C. DLS data were obtained on a Viscotek 802-100 dynamic light scattering analyser at 25 °C. N_2 adsorption/desorption isotherms were measured at 77 K using an AUTOSORB-1-C system after the sample was first degassed at 120 °C overnight. Surface areas were determined by the BET method.

Results and discussion

Gelatin was selected as a growth matrix as it is inexpensive and non-toxic, forms thermoreversible gels and its proteinaceous composition ensures abundant functionality is present from multiple amino-acid side chains (*e.g.* aspartates and glutamates) for interaction with MOF building blocks. Further, gelatin is water soluble without addition of acid or base which would be incompatible with many coordination-based frameworks. For the growth of MOFs in gelatin hydrogels two routes were taken as illustrated in Scheme 1 for HKUST-1. Route (a) involved sequential diffusion of the metal ions and ligands into a pure gelatin hydrogel whereas route (b) employed a homogeneous preformed M(II)@gelatin (M = Zn, Cu) precursor gel.[14]

ZIF-8@gelatin composites

Hydrogels containing 5 wt% pure gelatin were first cast as 10 × 4 mm cylindrical pellets by pipetting hot gelatin solutions into drinking straws sealed at one end and allowing to cool (Fig. 1a). To form ZIF-8@gelatin hydrogel composites by route (a) (Scheme 1), the gelatin pellets were first soaked overnight in an aqueous zinc nitrate solution (0.0168 M) followed by washing and soaking in an ethanolic solution of 2-methylimidazole (2-MeIm) such that the Zn(II) : 2-MeIm ratio of the solution

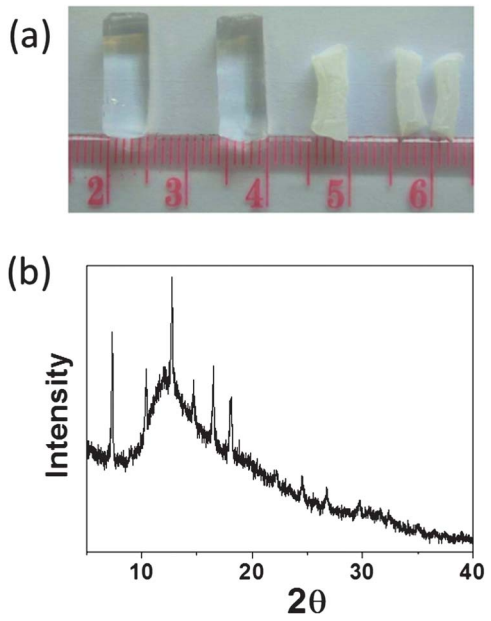

Fig. 1 (a) digital photographs of (L–R): 5 wt% gelatin pellet; Zn(II)@gelatin precursor pellet; ZIF-8@gelatin composite prepared by soaking in ethanolic 2-MeIm solution; cross-section of ZIF-8@gelatin pellet. (Ruler scale in cm) (b) PXRD pattern of ZIF-8@gelatin composite – the large amorphous background arises from the gelatin component.

concentrations was 1 : 40 – a typical ratio suitable for nanoscale ZIF-8 growth from aqueous mixtures. After 24 h the clear gel pellets became opaque (Fig. 1a) indicating ZIF-8 formation, which was confirmed by powder X-ray diffraction (PXRD). However, ZIF-8 formation was not restricted to the hydrogel matrix and the pellets were observed to have a coating of the framework on their exterior surface as well as bulk formation in solution. This suggests that hydrated Zn(II) ions did not adequately penetrate into the hydrogel following initial soaking, and/or are relatively mobile within the gel matrix itself. This is similar to the growth of large crystals of Zn(HBTC)(pyr)2·EtOH (pyr = pyridine) in PEO (polyethyleneoxide) organogels, where crystal growth is limited to the gel–solution interface.[15]

In order to confine ZIF-8 formation within the hydrogel we prepared a homogeneous Zn(II)@gelatin precursor gel by adding 100 mg of $Zn(NO_3)_2 \cdot 6H_2O$ to the 5 wt% gelatin sol prior to casting into pellets (Fig. 1a), as outlined in route (b) shown in Scheme 1. This permits a more controlled synthesis of ZIF-8@gelatin composites using pellets containing known amounts of metal ions. Zn(II)@gelatin pellets were soaked in ethanolic 2-MeIm (1 : 40) overnight, as previously outlined. As shown in Fig. 1a the colourless Zn(II)@gelatin pellets turned opaque and were observed to shrink in size upon soaking, which is common for gelatin hydrogels exposed to alcoholic solvent mixtures (Fig. S1†). Successful ZIF-8 formation was confirmed by PXRD after freeze-drying of the pellets (Fig. 1b), and there was significantly less precipitation of bulk ZIF-8 when the precursor gel is employed. By contrast, the use of a 2-MeIm@gelatin precursor gel led only to bulk ZIF-8 formation, indicating the imidazole linker is significantly more mobile than Zn(II) within the hydrogel matrix.

Thermogravimetric analysis (TGA) of freeze-dried ZIF-8@gelatin pellets reveals the composite decomposes gradually over the temperature range 120–675 °C with a decomposition profile reminiscent of pure gelatin (Fig. S2†). The residual ZnO at 800 °C indicates a ZIF-8 loading of 39.7 wt%, which is comparable to the ZIF-8@chitosan composites recently reported by Yao *et al.*[10a] Rheology measurements (Fig. S3†) indicate the presence of ZIF-8 particles modestly increase the strength of the hydrogel matrix. The storage modulus, G', for the ZIF-8@gelatin composite is 5 times higher than gelatin alone, and there is no apparent gel melting temperature over the range studied compared to a melting temperature of 38 °C for pure gelatin. This reveals the ability of MOF crystallites to alter the mechanical properties of biologically derived hydrogels, as previously observed for gelatin–clay composites[16] and MOF crystals dispersed in monomer solutions prior to polymerisation-induced hydrogel formation.[17]

The composite pellets are readily dispersed in hot water (Fig. 2 inset), and following dilution and cooling, were examined by dynamic light scattering (DLS) (Fig. S4†). After reaction (soaking) for 24 h, the majority of the particles upon redispersion fell within a distribution centred at 205 ± 32 nm: this size relates to the ZIF-8 particle plus gelatin bound to the surface. The dispersions are also extremely stable, with little or no precipitation observed after 2 months (Fig. 2 inset) indicating their suitability for biologically relevant applications. Further, the particle size distribution of 195 ± 36 nm determined by DLS (Fig. S4†), clearly demonstrates that the particles did not aggregate over this time period, stabilised by interaction with the soluble macromolecular network. Similar stability has been reported for acidic colloidal dispersions of nanoscale cyanometallate networks grown within preformed chitosan beads.[10b]

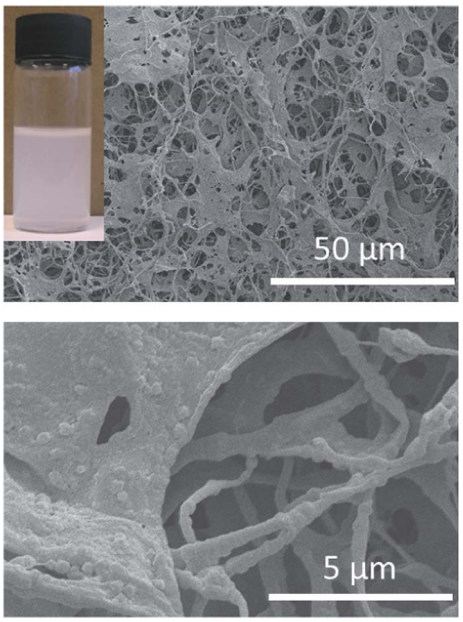

Fig. 2 SEM images of a freeze-dried dispersion of ZIF-8@gelatin. The digital photograph inset in the top image shows the aqueous dispersion after standing on the bench for two months.

The (re)dispersions were freeze-dried and examined by SEM, which showed that the ZIF-8 crystals were homogeneously embedded throughout the fibrous hydrogel network (Fig. 2). N_2 adsorption isotherms revealed an almost linear uptake at 77 K, with a hysteretic desorption profile across the whole pressure range (Fig. S5†). This is attributed to the gelatin matrix only, and the apparent BET surface area of 123 $m^2 g^{-1}$ is significantly lower than expected based on the determined ZIF-8 contents, as previously reported for ZIF-8@chitosan composites.[10a] This is entirely consistent with the SEM images in Fig. 2, where ZIF-8 particles are clearly covered by the hydrogel blocking access to the micropores, and further confirmed by TEM (Fig. S6†) where aggregates of ZIF-8 particles have residual gelatin strongly associated with them.

It is possible however to remove the biopolymer component from the ZIF-8@gelatin composites by repeated washing and centrifugation in water at 90 °C. The high water stability of the framework allows the recovery of phase pure ZIF-8 as evidenced by PXRD (Fig. S7†) and displays a significantly reduced amorphous background in the absence of gelatin. The BET surface area of the recovered ZIF-8 is 1350 $m^2 g^{-1}$ (Fig. S8†), which indicates that all gelatin has been removed. This observation confirms further the successful preparation of the open framework structure within the hydrogel matrix and the role of the latter in blocking its microporosity.

We investigated the role of concentration and time on ZIF-8 particle size within gelatin matrices. We first prepared Zn(II)@gelatin precursors containing low loadings of Zn (5–40 mg), and after soaking in ethanolic 2-MeIm, pellet opacity increased with Zn contents (Fig. S9†) consistent with greater ZIF-8 deposition. A similar observation is made for precursor pellets of fixed Zn(II) contents over time, which shrank to a greater degree with increased EtOH exposure (Fig. S9†).

Dispersed slices of the composite pellets were examined by DLS, and in all cases multiple size distributions ranging from nm to μm were recorded even at low levels of Zn(II) inclusion or after short time intervals (Tables S1 and S2†). DLS measurements of gelatin-only sols of the same highly dilute concentration revealed no protein aggregation, thus all observed size distributions are attributable to ZIF-8@gelatin composites. The redispersed ZIF-8 particles are not as small or monodisperse as in previous reports using small molecule additives[18] or addition of organo-soluble polymers such as polyethyleneimine,[19] which is clearly related to the composition and structure of the gelatin hydrogel growth matrices under the specific conditions investigated. For example, complex coordination and deprotonation equilibria are likely to result from the diversity of acidic and basic functionality expressed by the amino-acid side chains in gelatin, which will influence nucleation and growth processes.[18] Further, the physical properties of the gels will differ with starting Zn contents, pH and EtOH exposure that could affect diffusion of the 2-MeIm linker into the hydrogel matrix; diffusion rates and pathways could thus potentially change during the course of an experiment. The larger particles likely result from aggregation of smaller (primary) particles following multiple nucleation events within the gel cavities and/or from ZIF-8 growth on the exterior of the pellets, perhaps driven by a combination of the factors described. Upon redispersion, the ZIF-8 particles will also have varying amounts of surface gelatin which will influence the observed size distributions. These results are in contrast to the those above, where a starting Zn(II) contents of 100 mg resulted in a relatively narrow size distribution of ZIF-8 particles. This suggests that there is an optimum Zn(II) : gelatin ratio if monodisperse particles are to be obtained.

HKUST-1@gelatin composites

Growth of the carboxylate-based framework HKUST-1 in gelatin matrices was also investigated to determine the scope of the approach. A 5 wt% pure gelatin hydrogel pellet was first soaked in aqueous $Cu(OAc)_2$, followed by an aqueous solution of Na_3BTC. The colourless pellets initially turned blue, and became opaque and lighter in colour after immersion in the ligand solution (Fig. 3, inset). This is consistent with HKUST-1 deposition, which was confirmed by PXRD (Fig. S10†), and less shrinkage was observed than in the ZIF-8 case where EtOH was used to solubilise the ligand. Interestingly, it was not necessary to first prepare a Cu(II)@gelatin precursor gel (route (b), Scheme 1) to limit MOF deposition outside of the pellet as required for ZIF-8@gelatin composites. This is consistent with reduced mobility of Cu(II) within the hydrogel through stronger interaction with the amino-acid side chains of the gelatin matrix as reflected in the stability constants of amino-acid complexes of these metal ions.[20]

This is a wholly aqueous synthesis of HKUST-1 at room temperature, and despite reports of the competing phases $[Cu(HBTC)(H_2O)_3]$, $[Cu_2(BTC)(OH)(H_2O)]$ and $[Cu(H_2BTC)_2(H_2O)_2]\cdot 3H_2O$ being favoured in syntheses containing high water contents,[21] these appear to be suppressed by the gelatin matrix in the present case. Furthermore, direct reaction between $Cu(OAc)_2$ and Na_3BTC in water in the absence of the hydrogel does not yield HKUST-1, rather a mixed phase of one or more of the other known Cu-BTC materials alongside other impurities (Fig. S11†). During the course of our study we have found that the aqueous synthesis of HKUST-1 is pH

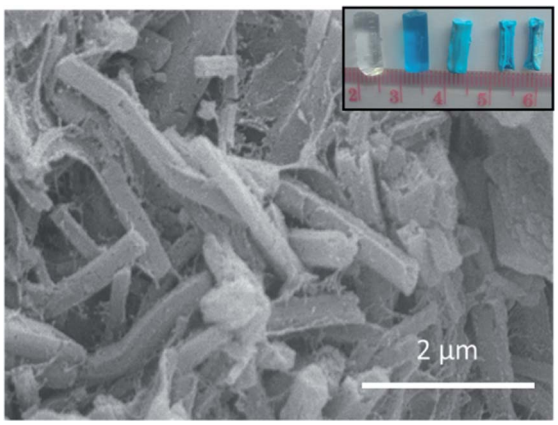

Fig. 3 SEM image of rod-like crystals of HKUST-1 prepared within a gelatin hydrogel matrix. The inset shows (L–R): 5 wt% gelatin pellet; the same pellet after soaking in aqueous $Cu(OAc)_2$; HKUST-1@gelatin composite; cross-section of HKUST-1@gelatin pellet. (Ruler scale in cm).

sensitive, and does not readily form above pH 5.5. The pH of the Na_3BTC ligand solution exceeds this value, so in the present case it is highly likely that the abundant acid–base functionalities present in the gelatin matrix act as a buffer to regulate pH thus permitting MOF formation only within the chemically controlled hydrogel environment under these conditions.

Cross-sections of the freeze-dried pellets were examined by SEM which revealed μm-sized rod-like crystals of HKUST-1 had formed within the hydrogel matrix as shown in Fig. 3. Although, HKUST-1 has been prepared in numerous ways,[6] the crystals invariably adopt an octahedral morphology whether the MOF is configured as thin films, confined at the nanoscale, grown onto porous scaffolds, or prepared in the presence of polymers. To the best of our knowledge this is the first report of HKUST-1 with a microrod morphology, which is clearly driven by the presence of the gelatin matrix. This is directly analogous to matrix-mediated biomineralisation processes,[1,22] since both the crystal growth chemistry and morphology is directly influenced by the hydrogel.

Recent studies of HKUST-1 crystal growth probed by *in situ* AFM[23] reveal that growth occurs *via* addition of hydrated monomer combinations to crystal surfaces, implying that the functional groups at the hydrogel interface cap or interact with specific crystal faces promoting anisotropic growth. While oriented growth of HKUST-1 has previously been observed on mono-functionalised carboxylate and hydroxyl terminated self-assembled monolayers on Au substrates,[24] the specific functionality leading to microrod growth within gelatin is much less clear. Despite this, HKUST-1 constitutes an excellent model system to further investigate the role of biologically derived hydrogels on the crystal growth of MOFs and will form the basis of future investigations.

The bulk HKUST-1@gelatin composites were further characterised by TGA and N_2 adsorption. Despite relatively high MOF contents of 70%, the freeze-dried composite pellets were essentially non-porous to N_2 at 77 K indicating the outer surface of the HKUST-1 microrods are covered by gelatin preventing access to the 3-dimensional micropore structure. Due to the relative instability of HKUST-1 in hot water, it was unfortunately not possible to remove the biopolymer from the HKUST-1@gelatin composites to completely isolate the HKUST-1 microrods since the framework transforms into another phase under these conditions.

Gelatin as a macromolecular additive

It is clear that gelatin hydrogel matrices are excellent for enhancing the aqueous stability of colloidal MOFs and have the ability to control growth and influence crystal morphology analogous to natural biomineralisation processes. To further investigate the effect of gelatin on MOF crystal growth, we have employed this in small quantities (≤1 wt%) as a soluble macromolecular additive. There are very few studies of this type,[19,25] especially for the aqueous synthesis of MOFs.

We added small amounts of gelatin (0.005–0.1 wt%) to hydrothermal ZIF-8 syntheses at 120 °C and examined the crystal shape and size by SEM (Fig. 4). In all cases, phase pure ZIF-8 was formed as confirmed by PXRD (Fig. S12†). Overall,

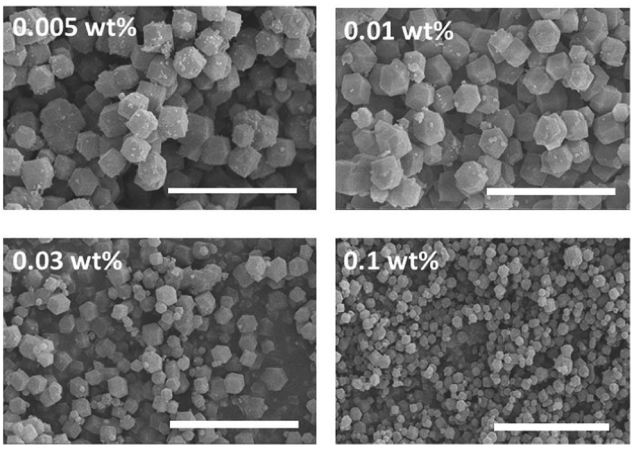

Fig. 4 SEM images of ZIF-8 prepared in aqueous solution at 120 °C in the presence of small amounts of gelatin (0.005–0.1 wt%) as a macromolecular crystal growth modifier. Scale bar in all images is 10 μm.

addition of gelatin tends to reduce the ZIF-8 crystal size which becomes more pronounced with increasing gelatin content (Fig. 4 and Table S3†). In this way we are able to reduce crystal size from ~3.0 μm (without gelatin) to 2.1 ± 1.0 μm, 1.0 ± 0.2 μm and 300 ± 90 nm when 0.005, 0.03 and 0.1 wt% of gelatin is present, respectively. While this indicates only small amounts of gelatin are required to reduce particle size, the distributions remain relatively large (±25%) when compared to previous work with ZIFs.[18,19,26] Again, we attribute this to the diverse functionality and resulting complex solution behaviour of gelatin when compared to small molecule and monofunctional polymeric additives. In contrast to ZIF-8@gelatin composites prepared by *in situ* growth, N_2 adsorption yields type I isotherms and high apparent BET surface areas (Fig. S13†) consistent with the preservation of ZIF-8 microporosity when the framework is synthesised in the presence of small amounts of added gelatin.

We also investigated the effect of gelatin on HKUST-1 crystal size. Given the difficulties preparing this framework in pure water (Fig. S11†), gelatin was added to standard solvothermal HKUST-1 syntheses in 50 : 50 EtOH–H_2O solvent mixtures. PXRD indicates that HKUST-1 is readily formed in the presence of gelatin up to 1 wt% (Fig. S14†), and SEM reveals aggregates of HKUST-1 particles form mesostructured assemblies (Fig. 5a). Similar supraparticle networks of HKUST-1 nanoparticles have previously been reported for the rapid addition of solutions of the metal ions and framework-forming ligands under ambient conditions.[27] The particle size within our HKUST-1 mesostructures derived from SEM images are 1.9 ± 1.0 μm in the presence of 0.1 wt% gelatin (Fig. S15†), which are reduced to 65 ± 20 nm at 1 wt% gelatin indicating that the biopolymer acts as an effective modifier to control particle size as also observed for ZIF-8. This affords a level of control not accessible by simple mixing of the components.

The function of gelatin as modifier in this case compares very well to the use of dodecanoic acid as a monocarboxylate coordination modulator for HKUST-1 growth, where particle size can be tuned between 20 nm and 2 μm by controlling the nucleation process.[28] This may indicate that the carboxylate side chains of

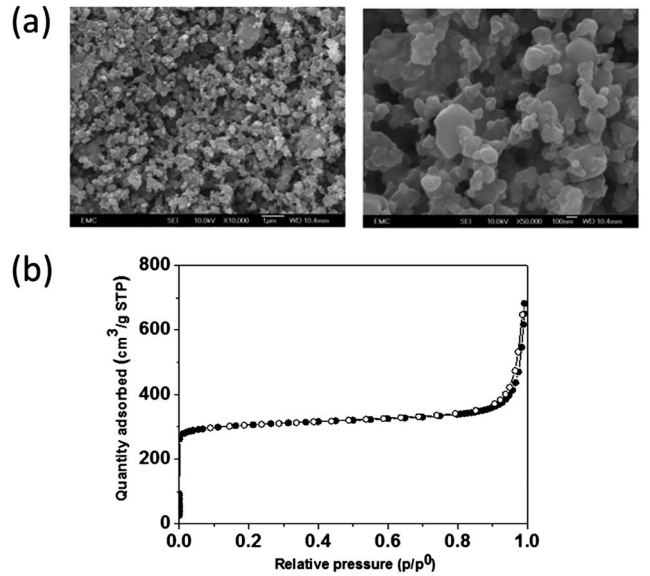

Fig. 5 (a) SEM images of HKUST-1 prepared solvothermally in EtOH–H_2O (1 : 1) in the presence of 1 wt% gelatin, revealing the mesostructured assemblies of MOF nanoparticles. (b) Nitrogen adsorption isotherm of the sample shown in (a) measured at 77 K.

glutamate and aspartate residues within the gelatin matrix play a similar role. The mesostructuring of HKUST-1 was clear from N_2 adsorption isotherms, which were intermediate type I/IV in shape (Fig. 5b) with significant uptake and desorption hysteresis in the range $p/p^0 = 0.8$–1.0 consistent with the interparticle voids observed by SEM. The sample prepared using 1 wt% gelatin has an apparent BET surface area of 1208 $m^2\ g^{-1}$, which is slightly higher than that recorded for the bulk sample. It displays a broad BJH pore size distribution centred at 70 nm and extending into the macropore regime arising from the particle interstices, as well as micropores from the MOF itself.

Conclusion

In conclusion, we have applied a biomineral-inspired approach to the preparation of prototypical MOFs within gelatin hydrogel matrices. This work confirms the importance of functional biologically derived macromolecules to the aqueous dispersibility and colloidal stability of MOFs, and clearly demonstrates their influence on crystal size and morphology. Further, the MOF@gelatin composites are likely to have increased biocompatibility enhancing their potential in biological applications. While the mechanisms governing growth and interaction of MOF crystals within proteinaceous scaffolds appear complex and not yet understood, MOF@protein composites are highly relevant to the application of MOFs in biological systems, and further study in this direction is essential.

Acknowledgements

We gratefully acknowledge funding by the European Research Council (ERC) under contract number ERC-StG-2010-BIOMOF-258613. We also thank Dr Dave Adams and Dr Lin Chen (Liverpool) for assistance with rheology measurements.

Notes and references

1 S. Mann, *Biomineralisation: principles and concepts in bioinorganic materials chemistry*, OUP, 2001.
2 E. Asenath-Smith, H. Li, E. C. Keene, Z. W. She and L. A. Estroff, *Adv. Funct. Mater.*, 2012, **22**, 2891.
3 S. Busch, U. Schwarz and R. Kniep, *Adv. Funct. Mater.*, 2003, **13**, 189.
4 A. Ethirajan, U. Ziener, A. Chuvilin, U. Kaiser, H. Cölfen and K. Landfester, *Adv. Funct. Mater.*, 2008, **18**, 2221.
5 (*a*) S. Kitagawa, R. Kitaura and S. Noro, *Angew. Chem., Int. Ed.*, 2004, **43**, 2334; (*b*) G. Férey, *Chem. Soc. Rev.*, 2008, **37**, 191; (*c*) C. Janiak and J. K. Vieth, *New J. Chem.*, 2010, **34**, 2366.
6 MOF special issue, *Chem. Soc. Rev.*, 2009, **38**, 1201 (19 articles).
7 (*a*) E. A. Flügel, A. Ranft, F. Haase and B. V. Lotsch, *J. Mater. Chem.*, 2012, **22**, 10119; (*b*) A. Carne, C. Carbonell, I. Imaz and D. Maspoch, *Chem. Soc. Rev.*, 2011, **40**, 291.
8 N. Stock and S. Biswas, *Chem. Rev.*, 2012, **112**, 933.
9 T. Tsuruoka, S. Furukawa, Y. Takashima, K. Yoshida, S. Isoda and S. Kitagawa, *Angew. Chem., Int. Ed.*, 2009, **48**, 4739.
10 (*a*) J. Yao, R. Chen, K. Wang and H. Wang, *Microporous Mesoporous Mater.*, 2013, **165**, 200; (*b*) Y. Guari, J. Larionova, M. Corti, A. Lascialfari, M. Marinone, G. Poletti, K. Molvinger and C. Guérin, *Dalton Trans.*, 2008, 3658.
11 R. Blom, I. M. Dahl and A. I. Spjelkavik, *Brit. UK Pat. Appl.*, 2012, GB 2490473 A 20121107.
12 K. S. Park, Z. Ni, A. P. Cote, J. Y. Choi, R. Huang, F. J. Uribe-Romo, H. K. Chae, M. O'Keeffe and O. M. Yaghi, *Proc. Natl. Acad. Sci. U. S. A.*, 2006, **103**, 10186.
13 S. S.-Y. Chui, S. M.-F. Lo, J. P. H. Charmant, A. G. Orpen and I. D. Williams, *Science*, 1999, **283**, 1148.
14 A. Schödel, C. Scherb and T. Bein, *Angew. Chem., Int. Ed.*, 2010, **49**, 7225.
15 O. M. Yaghi, G. Li and H. Li, *Chem. Mater.*, 1997, **9**, 1074.
16 Y. Q. Rao, *Polymer*, 2007, **48**, 5369.
17 R. Ananthoji, J. F. Eubank, F. Nouar, H. Mouttaki, M. Eddaoudi and J. P. Harmon, *J. Mater. Chem.*, 2011, **21**, 9587.
18 J. Cravillon, R. Nayuk, S. Springer, A. Feldhoff, K. Huber and M. Wiebcke, *Chem. Mater.*, 2011, **23**, 2130.
19 Y.-S. Li, H. Bux, A. Feldhoff, G.-L. Li, W.-S. Yang and J. Caro, *Adv. Mater.*, 2010, **22**, 3322.
20 P. S. Hallman, D. D. Perrin and A. E. Watt, *Biochem. J.*, 1971, **121**, 549.
21 (*a*) J. Gascon, S. Aguado and F. Kapteijn, *Microporous Mesoporous Mater.*, 2008, **113**, 132; (*b*) M. Schlesinger, S. Schulze, M. Hietschold and M. Mehring, *Microporous Mesoporous Mater.*, 2010, **132**, 121; (*c*) Y. K. Seo, G. Hundal, I. T. Jang, Y. K. Hwang, C. H. Jun and J. S. Chang, *Microporous Mesoporous Mater.*, 2009, **119**, 331.
22 S. Weiner and W. Traub, *Philos. Trans. R. Soc., B*, 1984, **304**, 425.
23 M. Shoaee, M. W. Anderson and M. P. Attfield, *Angew. Chem., Int. Ed.*, 2008, **47**, 8525.

24 E. Biemmi, C. Scherb and T. Bein, *J. Am. Chem. Soc.*, 2007, **129**, 8054.
25 (*a*) D. Jiang, T. Mallat, F. Krumeich and A. Baiker, *Catal. Commun.*, 2011, **12**, 602; (*b*) T. Uemura, Y. Hoshino, S. Kitagawa, K. Yoshida and S. Isoda, *Chem. Mater.*, 2006, **18**, 992.
26 Y. Pan, D. Heryadi, F. Zhou, L. Zhao, G. Lestari, H. Su and Z. Lai, *CrystEngComm*, 2011, **13**, 6937.
27 H. Du, J. Bai, C. Zuo, Z. Xin and J. Hu, *CrystEngComm*, 2011, **13**, 3314.
28 S. Diring, S. Furukawa, Y. Takashima, T. Tsuruoka and S. Kitagawa, *Chem. Mater.*, 2010, **22**, 4531.